EG UK Theory and Practice of Computer Graphics (2009)
Wen Tang, John Collomosse (Editors)

Uncertain Flow Visualization using LIC

R. S. Allendes Osorio[†1,2] and K. W. Brodlie[1]

[1]School of Computing, University of Leeds, United Kingdom
[2]Departamento de Computación, Facultad de Ingeniería, Universidad de Talca, Chile

Abstract

In this paper we look at the Line Integral Convolution method for flow visualization and ways in which this can be applied to the visualization of two dimensional, steady flow fields in the presence of uncertainty. To achieve this, we start by studying the method and reviewing the history of modifications other authors have made to it in order to improve its efficiency or capabilities, and using these as a base for the visualization of uncertain flow fields. Finally, we apply our methodology to a case study from the field of oceanography.

1. Introduction

All data is uncertain by nature, whether it comes from errors made when taking measurements on the field or from errors generated by computer simulations. Despite this, it is not uncommon that, when it comes to visualization, data is considered to be exact, and images are produced under that assumption.

There are areas though, where the uncertainty is a fundamental property of the data, and if not considered, visualization results can not be considered valid. For example, take the case when an underlying physical model is in itself uncertain, and therefore a number of simulations are needed in order to correctly understand the phenomenon. In such a case, we no longer have a single 'result' to use as input for our visualization techniques, but a series of plausible results, each one with its own probability of being correct.

In scientific applications, vector fields are usually described using two quantities defined over a grid: magnitude and direction. In the uncertainty visualization case, magnitude and direction are not represented as precise values, but as random variables, with associated Probability Density Functions (PDF). For a random variable X, the PDF, f_X tells us that the probability of X lying in the interval $[a,b]$ is given by:

$$\int_a^b f_X(x)dx \tag{1}$$

Assuming it is possible to find the PDFs that define the behaviour of the magnitude and direction of each vector in a field, in this paper we look at the problem of how to visualize them, and how this problem can be approached by considering the modification or augmentation of traditional flow visualization techniques.

In Section 2, we will provide a brief introduction to flow visualization algorithms and how there have been efforts to apply these within the uncertain visualization context. In Section 3 we look in more detail at the Line Integral Convolution algorithm (LIC), vital to our approach for uncertain flow visualization. Section 4 defines the methodology we will follow in order to implement an uncertain version of the Line Integral Convolution method. In Section 5 we introduce some of the statistical processes we have used in order to derive an uncertain flow field from a multivalue dataset. In Section 6 we present the results of applying our approach to a case study from the field of oceanography. And finally, in Section 7, we draw conclusions from our work and comment on future developments.

2. Background and Related Work

The visualization of both static and dynamic flow fields is a problem scientists from different areas of knowledge often have to face. In consequence, several techniques have been developed to address the issue, and approaches such as "streamlines" or "particle tracing" are widely known.

Not intending to provide an extensive review of the flow

† scsrsao@leeds.ac.uk

DOI: 10.2312/LocalChapterEvents/TPCG/TPCG09/215-222

visualization field, in this section we will introduce the efforts that have been made in the specific area of visualizing uncertain flows. For a good review of the state of the art in flow visualization, see [LHD*04].

In terms of uncertainty visualization, a good description of techniques applied specifically in the area of geographical data can be found in [MRH*05] and a general review of the current state of the art can be found in [LPK05]. Our own work, on visualizing uncertainty in contouring, was presented at EGUK08 [AOB08].

Next, we will look at some of the work that has been done in the specific area of uncertain flow visualization. We will also review a particular group of flow visualization techniques based on the use of textures, as these will give us the starting point for our approach to uncertain flow visualization.

2.1. Uncertain Flow Visualization

As mentioned before, uncertainty in the visualization process can arise at different stages [PWL97]. When data is collected, uncertainty can arise from the measurement instruments themselves or the numerical methods used in the data generation stage. Uncertainty is also generated by the algorithms that transform the data, when new variables for example are derived from the original measurements. Finally, the visualization process itself is a source of uncertainty when, for example, different rendering methods are used.

Wittenbrink and his colleagues investigated the ways in which glyphs could be used for the visualization of uncertainty arising in both the data acquisition and the modelling stages. They followed two approaches, first, an overlapping approach by which properties such as colour, transparency and size of a glyph are modified to encode the uncertainty in the data; but focused in a second approach, in which glyphs are designed specifically to include uncertainty cues. Under this second approach, arrow-like glyphs are defined in such a way that, for example, magnitude uncertainty in a vector can be represented by drawing multiple arrow heads and direction uncertainty is represented by varying the shape of the arrows [WPL96].

Lodha and his colleagues developed UFLOW, a system that focuses on the visualization of the uncertainty that arises when different algorithms are used to calculate streamlines based on the same flow field. They do this by rendering the output of two different algorithms simultaneously and use visual structures, such as glyphs or streamlines, to represent the differences between them [LPSW96].

In a similar approach, Lopes and Brodlie focused on showing the uncertainty that arises when analysing the error created by different numerical integrations of the same particle tracing algorithm [LB99].

2.2. Texture-based flow visualization

Although the methods introduced in Section 2.1 do allow the visualization of certain types of uncertainty, these either present flow properties through the whole field, but only at discrete locations, or they show the continuous properties of the field, but for only a reduced number or even a single particle. Texture-based flow visualization algorithms, on the other hand, allow the dense and continuous representation of the underlying flow field.

In 1991, Van Wijk introduced *spot noise*, with the intention of using randomly generated textures for the visualization of scalar and vector fields over surfaces [vW91]. The idea behind the spot noise technique is that, by generating a number of spots, it is possible to create random textures that reflect the behaviour of the flow field. Spots are located randomly along the texture and their visual properties, size, shape, direction, the presence of patterns or different types of edges, can be modified according to the vector local field.

Van Wijk also introduced Image Based Flow Visualization (or IBFV) [vW02], a method that allows the visualization of unsteady flow fields using animation. To produce the frames that compose the animation, a starting image is advected using the flow field and then blended with a background image. The resulting image is later used as a starting point to produce the next frame in the animation.

Following the ideas of Van Wijk on spatial convolution and combining it with digital differential analyser line drawing techniques, Cabral and Leedom introduced one of the most used texture-based visualization techniques: the Line Integral Convolution [CL93]. At each pixel, a streamline is traced in both the forward and backward directions, a random noise texture field is then evaluated along this streamline and convolved with a filter to produce the intensity to be shown in the final image. The next section presents a more detailed description of LIC, as this technique will be the starting point for our approach in uncertain flow visualization.

3. Line Integral Convolution (LIC)

Cabral and Leedom noticed that, although some techniques for the visualization of vector fields existed at the time, these were not always suitable when dealing with very dense fields or when generalized to applications outside the traditional scientific visualization field. To address this issue, they developed a new, texture-based method for the visualization of flow fields known as Line Integral Convolution, or LIC [CL93].

LIC is based on the idea that visual properties at each pixel in the final image, can be determined by generating a kernel that describes the behaviour of the field around the current location and convolving this with an input texture.

To understand how LIC works, let us consider the case

of a two-dimensional, static flow field, described as vectors over a regular grid. First, we define a random noise input texture of the same size as the input vector field. Then for each vertex in the input dataset, we calculate a streamline that defines the movement a particle would experience when exposed to the flow in both the forward and backward directions. Secondly, we convolve the streamline with the random input texture, using the length of the path as convolution kernel, in order to determine the intensity at the corresponding pixel in the final image.

Although results from this method are visually appealing, originally, LIC was a computationally expensive algorithm, that required numerous computations of streamlines along the flow field. Stalling and Hege [SH95] noticed that, for pixels that lie along a particular streamline, the results from the convolution process differ only by two small correction terms, one at each end of the streamline. So, if we generate a streamline longer than the kernel needed for the convolution process, the performance of the algorithm can be improved in two ways: by moving along the streamline and recursively calculating the intensity in the final image; and by reducing the number of streamlines that need to be generated.

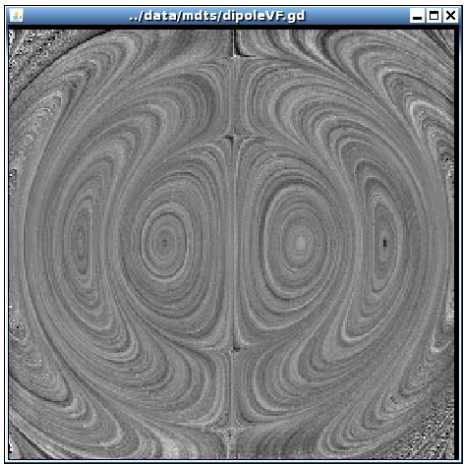

Figure 1: *Vector field generated by an irradiating dipole antenna, visualized using our implementation of the fast LIC algorithm and a white noise input layer.*

Figure 1 shows the results of using our implementation of the fast LIC algorithm to visualize the vector field generated by an irradiating dipole antenna (Vector field data obtained from IRIS Explorer).

Having implemented the LIC algorithm, we will introduce in the next section ways in which this can be modified for the uncertain flow situation.

4. Our Approach - Uncertain Line Integral Convolution

We have seen how a texture-based visualization technique, LIC, can be used for the visualization of vector fields. In this section we will review the ways in which this basic algorithm can be modified so that it can be used for the visualization of uncertainty in the flow fields.

To achieve this, we will use two different approaches, the modification of the input texture used for the LIC convolution (Section 4.1), and the modification of visual properties, such as hue (Section 4.2) and brightness (Section 4.3).

In order to test our ideas, we need a dataset that has uncertainty measurements. To solve this, and in an effort to clarify, we have added an arbitrary value to represent the uncertainty in the magnitude at each vector in the dipole dataset presented in Figure 1. To add the uncertainty, we have divided the dataset into four areas, then, we assign to each grid point in the lower left area a PDF for its velocity magnitude, with mean equal to 1 (due to vector normalization) and standard deviation equal to 0.1. Vectors in other areas, ordered counter-clockwise from the first, were assigned standard deviation values of 0.4, 0.6 and 0.8 respectively.

4.1. Multi-Frequency noise

In order to encode information regarding the magnitude of the underlying vector field, Kiu and Banks introduced a modified version of LIC that used multi-frequency noise as input layer for the convolution process [KB96].

Using a frequency inversely proportional to the magnitude of the vector field has, in terms of representing the magnitude, the advantage of generating long, thicker streaks in areas of high speed and short, thin streaks in areas of low speed [KB96].

When looked at from the uncertainty visualization viewpoint, a low frequency input texture, and the corresponding blur effect in the final image, can be used to encode locations where the uncertainty in the input data makes it difficult, or in cases even impossible, to clearly define the flow direction.

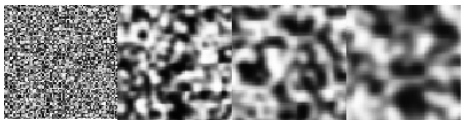

Figure 2: *Four different noise layers. From left to right, the original, high frequency, randomly generated white noise layer; and decreasing frequency layers generated using Gaussian filters and histogram equalization.*

Starting from a high frequency white noise image, lower frequency layers can be easily derived using Gaussian filters and histogram equalization [Eff00]. Figure 2 shows the results of such a process. For the initial high-frequency white noise layer, values are randomly generated at a ratio of one value per pixel. Moving from left to right, and following the lines of [KB96], correlated noise layers are calculated using

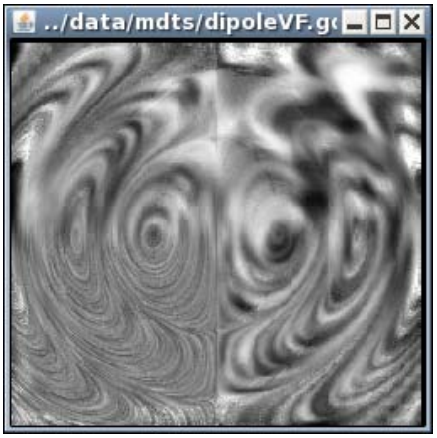

Figure 3: *Using a composition of multiple frequencies random noise, we can generate a new LIC image of our dipole dataset.*

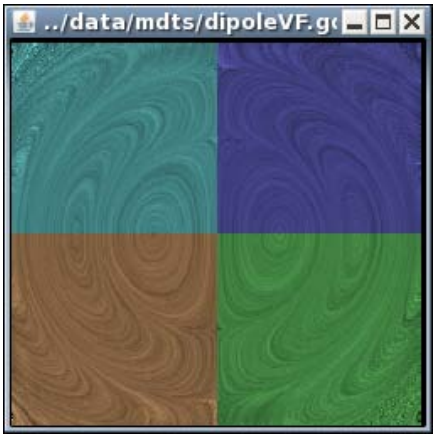

Figure 4: *Use of colour to show different values of uncertainty in our dipole dataset.*

Gaussian filters of size 5, 7 and 9, and histogram equalization.

When using multi-frequency input layers together with our LIC implementation, the lines that show the flow patterns become, as expected, increasingly blurred, thus giving the impression of a flow that is not well defined. Figure 3 shows the result of applying such an approach to our test dipole dataset.

4.2. Colour

Shen, Johnson and Ma used dye advection and animation to depict the direction of a flow being visualized using LIC [WJKM96]; similarly with the help of animation, and using decaying levels of intensity, Wegenkittl, Gröller and Purgathofer introduced an Oriented Line Integral Convolution (OLIC) [WGP97], and a more computationally effective version FROLIC [WG97]. Following a different approach, colour has also been used when working with multivalue datasets, in order to show multiple scalar magnitudes associated with a single vector field [UIM*03].

If we define each pixel in the final image as an HSV tuple, we can consider LIC as a method that only modifies the brightness of the pixel, or V-component of the model. This leaves us with two other components we can use to show the uncertainty in the dataset. We have chosen to use the Hue.

Figure 4 shows the results of using colour to identify different levels of uncertainty on the dipole dataset. This effect is achieved by evaluating the uncertainty at each pixel in the final image and using a mapping function to determine a hue value for the pixel. The pixel is finally drawn using the hue value selected from the colour mapping, a fixed value of saturation and the brightness level obtained from the LIC routine.

Notice that, although only four colours are shown in the image, these are mapped directly from the uncertainty values. This differs from the way uncertainty is mapped when using multiple noise layers, where a whole range of values is mapped to each of the different frequency noise layers.

4.3. Fog

There could be situations in which the most effective way to represent uncertainty is to actually avoid the display of highly uncertain data.

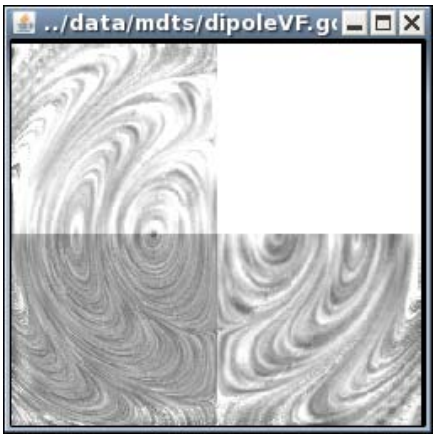

Figure 5: *Using a fog effect, we can effectively white out areas of high uncertainty in the dataset.*

To achieve this effect, we have implemented a fog effect that uses uncertainty to create a layer of high brightness that can be superimposed on the image resulting from the LIC routine. This is achieved by adding the levels of brightness of

the fog layer and the LIC image. Figure 5 shows the results of applying such a technique to the test dipole dataset.

5. Multivalued Velocity Fields

Let us assume we have a two dimensional, multivalued velocity field, i.e. there are several velocity values at each grid location. It is possible from this information, to derive statistics that define a probability density function (PDF) for both the magnitude and the direction of this field at each point in the grid. If we finally assume that the PDFs follow a normal (or Gaussian) distribution, then we can completely define them by calculating their means and standard deviations.

To calculate the statistics that define the PDF for the magnitude of a vector at each grid point, we use the following equations:

$$\bar{z} = \sum_{k=1}^{n} z_k \tag{2}$$

$$s = \sqrt{\frac{1}{n-1}\sum_{k=1}^{n}(z_k - \bar{z})^2} \tag{3}$$

where $\bar{z}$ is the mean vector magnitude at the current grid point, n represents the number of realizations available, z_k is the vector magnitude at the current location for realization k, and s is the standard deviation of the sample. Thus, we can say that the magnitude of the vector at each grid location is defined by a random variable X, with the distribution $N(\mu,\sigma)$ with $\mu = \bar{x}$ and $\sigma = s$.

The calculation of the statistics needed for the distribution of the direction is not as intuitive as the one for the magnitude, due to the circular nature in which angles are measured. However, there are references such as [Mar72] that provide us with an answer for this situation.

Let us define $\theta_1, \theta_2 \ldots \theta_k$ with $k : 1 \ldots n$ as the direction of the vector at each location in the grid for k-th realization. Then we can construct the following sums:

$$\begin{aligned} x &= \frac{1}{n}\sum_{k=1}^{n} cos\ \theta_k \\ y &= \frac{1}{n}\sum_{k=1}^{n} sin\ \theta_k \end{aligned} \tag{4}$$

We can re-write Equation 4 in polar coordinates:

$$x = r * cos\ \bar{\theta} \quad \text{and} \quad y = r * sin\ \bar{\theta} \tag{5}$$

with $0 \leq r \leq 1$ and $0^\circ \leq \bar{\theta} < 360^\circ$ by writing

$$r = \sqrt{x^2 + y^2} \quad \text{and} \quad tan\ \bar{\theta} = \frac{y}{x} \tag{6}$$

Finally, we can define $\bar{\theta}$ as the mean direction of the vector at the current location, as given by Equations 4 to 6. And we can define the standard deviation σ as

$$\sigma = \sqrt{-2 * ln\ r} \tag{7}$$

6. Results

In section 4, we described the methods we implemented for the visualization of uncertain flow, and applied them to a test dataset. In this section, we will present a real uncertain flow field from the field of oceanography, and present the results of using these previously described methods for its visualization.

6.1. Case Study: Oceanography

The study of the Ocean Dynamic Topography (ODT), which can be defined as the height of the sea surface above its rest state (the geoid), is of importance for oceanographers, as it allows them to understand the circulation patterns of oceans and the associated geostrophic surface currents, one of the main players in the regulation of Earth's climate.

However, technical difficulties in the definition of the geoid make it difficult to obtain direct measurements of the ODT, and scientists usually rely on alternative methods, such as the calculation of Mean Dynamic Topographies (MDT) to use in their studies. Bingham and Haines proposed a method to combine a series of MDTs to generate a composite MDT and use the spread among the original models as a formal measure of error [BH06].

Working together with the University of Reading, we have obtained the eight original MDTs used in the original derivation of the composite MDT. Each of these input models describes the height of the ocean using a regular two dimensional grid, in which the lowest-left grid point represent coordinates 41N 79W, and the upper-right grip point represents coordinates 77N 13E.

Using the method described in Section 5, we can use the eight original MDTs to generate an uncertain model of the flow field that represents the velocities at surface level.

Using the calculated mean velocity of the dataset as input to our normal LIC implementation, we obtain the results shown in Figure 6. Notice that areas where there is no defined data, due to large land-masses or islands, are blacked out on the final image.

Also, having derived measures for uncertainty in the magnitude and direction of the vector field, it is now possible to use the modified versions of LIC described in Section 4 to visualize this dataset.

6.2. Multi-frequency noise

For both magnitude and direction in the vector field, we can divide the whole range of uncertainty values into a series

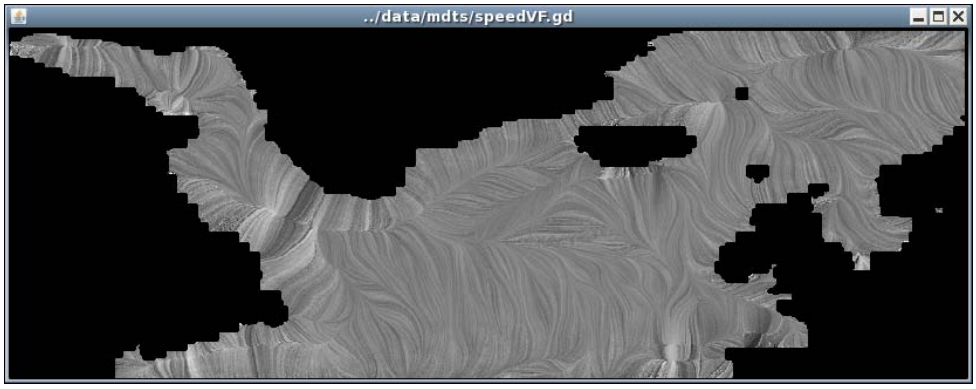

Figure 6: *Normal LIC representation of the gradient vector field derived from the composite MDT dataset.*

of discrete levels, and use these to select different layers of frequency noise to use in the convolution process of LIC as described in Section 4.1.

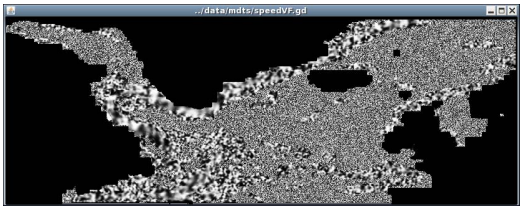

Figure 7: *Multi-frequency noise mask generated when using five levels of equally spaced magnitude uncertainty levels.*

In our case, we have chosen to divide the range into five equally spaced levels of uncertainty. For the magnitude case, this generates an input noise mask as shown in Figure 7.

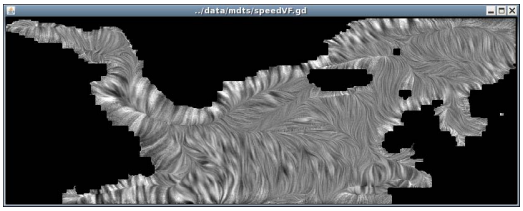

Figure 8: *Multi-frequency LIC representation of the composite MDT gradient dataset, using magnitude uncertainty to generate the input noise layer mask.*

In turn, Figures 8 and 9 show the results of using our multi-frequency LIC to visualize the uncertainties in both magnitude and direction of the flow field.

6.3. Colour Addition

As described in section 4.2, we can also use colour to encode information regarding the uncertainty in our flow field.

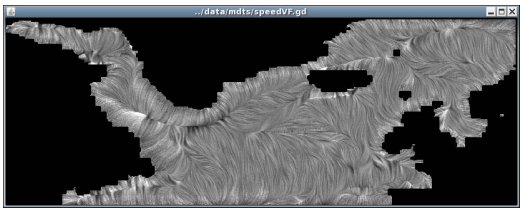

Figure 9: *Multi-frequency LIC representation of the composite MDT gradient dataset, using direction uncertainty to generate the input noise layer mask.*

Figure 10 shows a basic LIC image, in which we have used colour to represent the uncertainty in the magnitude of each vector in the field. Notice that for mapping purposes, the uncertainty range has been normalized to the interval (0,1), and that as mentioned in Section 4.2, the colour mapping is a continuous function of the uncertainty values.

At this point, it is possible to start incorporating different techniques into our visualization. These can be used redundantly to encode the same information and produce a stronger effect, or as an option to add more information to our visualization.

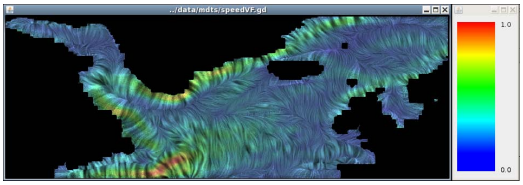

Figure 11: *Multi-frequency and colour LIC. Colour is used to encode the magnitude of vectors, whilst the uncertainty in the magnitude is used to select the noise layer to be used in the convolution process.*

Figures 11 and 12 show two different ways in which

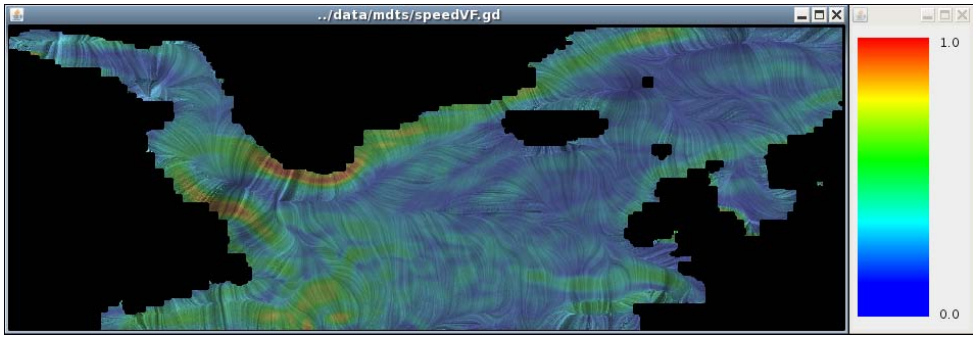

Figure 10: *Normal LIC representation of the gradient vector field composed with a colour map of the magnitude's uncertainty.*

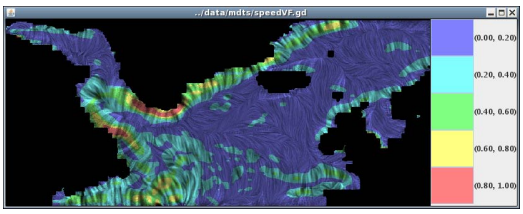

Figure 12: *Multi-frequency and colour LIC image. Noise layers are selected based in the uncertainty in magnitude. Colour is also used to identify the noise layer being used at the current location.*

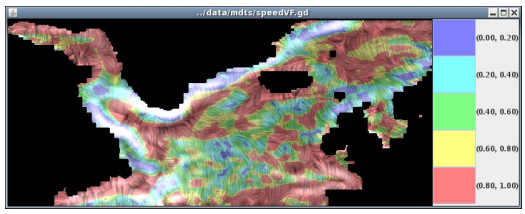

Figure 14: *Colour and multi-frequency noise layers are used to show the uncertainty in the direction of the field. The fog layer used is based in the magnitude's uncertainty.*

colour can be incorporated when using multi-frequency noise with LIC. First, in Figure 11 we use colour to map the magnitude of the vector field (which has also been normalized to the interval (0,1)) whilst a multi-frequency noise layer has been constructed using the *uncertainty* in the magnitude. Figure 12 on the other hand, both colour and multi-frequency noise are used to identify different levels of uncertainty in magnitude of the vector field.

6.4. Fog Effect

Finally, we can use the uncertainty, either in the magnitude or the direction of the vector field, to derive *fog layers* which can be used to increase the brightness in areas of high uncertainty in the final LIC image.

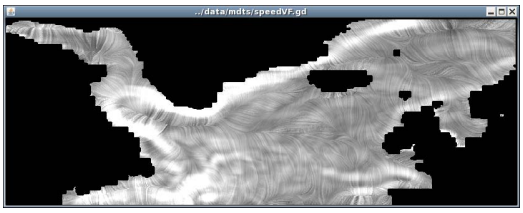

Figure 13: *Normal LIC image with increased brightness according to the uncertainty in vector's magnitude.*

As before, different techniques can be used to show a combination of different types of uncertainty, together with other properties of the vector field. Figure 14 shows the result of running multi-frequency LIC, using the uncertainty in the direction to select both the noise layers and the colour mapping, and using the uncertainty in the magnitude to create the fog effect.

7. Conclusions and Future Work

In this paper, we have reviewed two different approaches to modify the Line Integral Convolution algorithm, in order to make it suitable for the visualization of static, uncertain fluid flows. These are the use of multi-frequency random input layers, and the use of colour and brightness.

The described techniques have been implemented and applied to two datasets: a test dataset showing the field generated by an irradiating dipole antenna, with synthesized uncertainty; and a practical case study from the field of oceanography.

We have also shown that, through the combination of the different approaches, it is possible to show simultaneously the mean and the standard deviation of a particular component of the vector field; and that it is also possible to show different types of uncertainty in a single image.

We are currently experimenting with the modification of

other properties when generating the input layer used by LIC, in a continuous search for more ways to encode uncertainty information. One of these approaches is looking at the range of frequencies used when generating white noise and how this could be related to the uncertainty in the field.

In terms of the visualization algorithm, we are looking at implementing this techniques using a different texture-based visualization technique as starting point. In particular, we have taken the first steps towards an uncertain enabled version of van Wijk's technique Image Based Flow Visualization [vW02].

We have assumed a normal distribution, however, the ideas will apply to other distributions (such as uniform), and we hope to look at this in the future.

We are aware that further evaluation of the techniques is necesary in order to understand the perceptual issues better, and we are currently planning this.

8. Acknoledgements

We would like to acknowledge the help provided by Dr. Rory Bingham, Professor Keith Haines and Dr. Alastair Gemmell at the University of Reading in terms of providing the dataset used as case study for this report and for their help in reviewing our work and suggesting a number of improvements.

References

[AOB08] ALLENDES OSORIO R., BRODLIE K.: Contouring with uncertainty. In *Proceedings 6th Theory & Practice of Computer Graphics Conference(TP.CG.08)* (2008), Lim I. S., Tang W., (Eds.), Eurographics Association.

[BH06] BINGHAM R. J., HAINES K.: Mean dynamic topography: intercomparisons and errors. *Philosophical Transactions of The Royal Society A* (2006), 903 – 916.

[CL93] CABRAL B., LEEDOM L.: Imaging vector fields using line integral convolution. In *Proceedings of ACM SIGGRAPH 93* (1993), pp. 263–272.

[Eff00] EFFORD N.: *Digital Image Processing: a practical introduction using Java*. Addison-Wesley, 2000.

[KB96] KIU M.-H., BANKS D. C.: Multi-frequency noise for lic. In *VIS '96: Proceedings of the 7th conference on Visualization '96* (Los Alamitos, CA, USA, 1996), IEEE Computer Society Press, pp. 121–126.

[LB99] LOPES A., BRODLIE K.: Accuracy in 3D particle tracing. In *Mathematical Visualization: Algorithms, Applications and Numerics*, Hege H., Polthier K., (Eds.). Springer Verlag, 1999, pp. 329–341.

[LHD*04] LARAMEE R. S., HAUSER H., DOLEISCH H., VROLIJK B., POST F. H., WEISKOPF D.: The state of the art in flow visualization: Dense and texture-based techniques. *Computer Graphics Forum 23* (2004), 203–221.

[LPK05] LOVE A. L., PANG A. T., KAO D. L.: Visualizing spatial multivalue data. *IEEE Computer Graphics and Applications* (2005), 69–79.

[LPSW96] LODHA S. K., PANG A., SHEEHAN R. E., WITTENBRINK C. M.: UFLOW: Visualizing uncertainty in fluid flow. In *IEEE Visualization '96*, (1996), Yagel R., Nielson G. M., (Eds.), pp. 249–254.

[Mar72] MARDIA K.: *Statistics on Directional Data*. Academic Press, 1972.

[MRH*05] MACEACHREN A. M., ROBINSON A., HOPPER S., GARDNER S., MURRAY R., GAHEGAN M., HETZLER E.: Visualizing geospatial information uncertainty: what we know and what we need to know. *Cartography and Geographic Information Science 32*, 8 (2005), 139–160.

[PWL97] PANG A. T., WITTENBRINK C. M., LODHA S. K.: Approaches to uncertainty visualization. *The Visual Computer 13*, 8 (1997), 370–390.

[SH95] STALLING D., HEGE H.-C.: Fast and resolution independent line integral convolution. In *SIGGRAPH '95: Proceedings of the 22nd annual conference on Computer graphics and interactive techniques* (New York, NY, USA, 1995), ACM, pp. 249–256.

[UIM*03] URNESS T., INTERRANTE V., MARUSIC I., E L., GANAPATHISUBRAMANI B.: Effectively visualizing multi-valued flow data using color and texture. In *Proceedings of the 14th IEEE Visualization Conference (VIS'03)* (2003).

[vW91] VAN WIJK J. J.: Spot noise - texture synthesis for data visualization. In *SIGGRAPH '91: Proceedings of the 18th annual conference on Computer graphics and interactive techniques* (New York, NY, USA, 1991), ACM, pp. 309–318.

[vW02] VAN WIJK J. J.: Image based flow visualization. *ACM Trans. Graph. 21*, 3 (2002), 745–754.

[WG97] WEGENKITTL R., GRÖLLER E.: Fast oriented line integral convolution for vector field visualization via the internet. In *VIS '97: Proceedings of the 8th conference on Visualization '97* (Los Alamitos, CA, USA, 1997), IEEE Computer Society Press, pp. 309–316.

[WGP97] WEGENKITTL R., GRÖLLER E., PURGATHOFER W.: Animating flow fields: Rendering of oriented line integral convolution. In *Proceedings of Computer Animation 97* (1997), pp. 15–21.

[WJKM96] WEI H.-S., JOHNSON C. R., KWAN-MA L.: *Visualizing Vector Fields using Line Integral Convolution and Dye Advection*. Tech. rep., National Physics Laboratory, 1996.

[WPL96] WITTENBRINK C. M., PANG A. T., LODHA S. K.: Glyphs for visualizing uncertainty in vector fields. *IEEE Transactions on Visualization and Computer Graphics 2* (1996), 266–279.